



NASA Glenn Icing Research Tunnel: 2014 Cloud Calibration Procedure and Results

*Judith F. Van Zante
Glenn Research Center, Cleveland, Ohio*

*Robert F. Ide and Laura E. Steen
Sierra Lobo, Inc., Cleveland, Ohio*

*Waldo J. Acosta
Jacobs Technology, Cleveland, Ohio*

NASA STI Program . . . in Profile

Since its founding, NASA has been dedicated to the advancement of aeronautics and space science. The NASA Scientific and Technical Information (STI) program plays a key part in helping NASA maintain this important role.

The NASA STI Program operates under the auspices of the Agency Chief Information Officer. It collects, organizes, provides for archiving, and disseminates NASA's STI. The NASA STI program provides access to the NASA Aeronautics and Space Database and its public interface, the NASA Technical Reports Server, thus providing one of the largest collections of aeronautical and space science STI in the world. Results are published in both non-NASA channels and by NASA in the NASA STI Report Series, which includes the following report types:

- **TECHNICAL PUBLICATION.** Reports of completed research or a major significant phase of research that present the results of NASA programs and include extensive data or theoretical analysis. Includes compilations of significant scientific and technical data and information deemed to be of continuing reference value. NASA counterpart of peer-reviewed formal professional papers but has less stringent limitations on manuscript length and extent of graphic presentations.
- **TECHNICAL MEMORANDUM.** Scientific and technical findings that are preliminary or of specialized interest, e.g., quick release reports, working papers, and bibliographies that contain minimal annotation. Does not contain extensive analysis.
- **CONTRACTOR REPORT.** Scientific and technical findings by NASA-sponsored contractors and grantees.

- **CONFERENCE PUBLICATION.** Collected papers from scientific and technical conferences, symposia, seminars, or other meetings sponsored or cosponsored by NASA.
- **SPECIAL PUBLICATION.** Scientific, technical, or historical information from NASA programs, projects, and missions, often concerned with subjects having substantial public interest.
- **TECHNICAL TRANSLATION.** English-language translations of foreign scientific and technical material pertinent to NASA's mission.

Specialized services also include creating custom thesauri, building customized databases, organizing and publishing research results.

For more information about the NASA STI program, see the following:

- Access the NASA STI program home page at <http://www.sti.nasa.gov>
- E-mail your question to help@sti.nasa.gov
- Fax your question to the NASA STI Information Desk at 443-757-5803
- Phone the NASA STI Information Desk at 443-757-5802
- Write to:
STI Information Desk
NASA Center for AeroSpace Information
7115 Standard Drive
Hanover, MD 21076-1320



NASA Glenn Icing Research Tunnel: 2014 Cloud Calibration Procedure and Results

Judith F. Van Zante
Glenn Research Center, Cleveland, Ohio

Robert F. Ide and Laura E. Steen
Sierra Lobo, Inc., Cleveland, Ohio

Waldo J. Acosta
Jacobs Technology, Cleveland, Ohio

National Aeronautics and
Space Administration

Glenn Research Center
Cleveland, Ohio 44135

Acknowledgments

The authors would like to thank NASA's Aeronautics Test Program for funding this essential effort. Many thanks are also due to the other IRT Engineers: Seth Sederholm, Larry Becks, Mark Kubiak and Sean Currie; and the expert and very patient IRT Technicians: Joe August, Dave Bremenour, Jason Bryant, Paul Butterfield, Bill Magas, Rob Maibauer, Terry Mathes, Shaun McNea, Perry Vraja. Also thanks to Colin Bidwell, Mr. LEWICE3D, for running the collection efficiencies on the multi-wire elements.

Trade names and trademarks are used in this report for identification only. Their usage does not constitute an official endorsement, either expressed or implied, by the National Aeronautics and Space Administration.

Level of Review: This material has been technically reviewed by technical management.

Available from

NASA Center for Aerospace Information
7115 Standard Drive
Hanover, MD 21076-1320

National Technical Information Service
5301 Shawnee Road
Alexandria, VA 22312

Available electronically at <http://www.sti.nasa.gov>

NASA Glenn Icing Research Tunnel: 2014 Cloud Calibration Procedure and Results

Judith F. Van Zante
National Aeronautics and Space Administration
Glenn Research Center
Cleveland, Ohio 44135

Robert F. Ide and Laura E. Steen
Sierra Lobo, Inc.
Cleveland, Ohio 44135

Waldo J. Acosta
Jacobs Technology
Cleveland, Ohio 44135

Abstract

The results of the December 2013 to February 2014 Icing Research Tunnel full icing cloud calibration are presented. The calibration steps included establishing a uniform cloud and conducting drop size and liquid water content calibrations. The goal of the calibration was to develop a uniform cloud, and to generate a transfer function from the inputs of air speed, spray bar atomizing air pressure and water pressure to the outputs of median volumetric drop diameter and liquid water content. This was done for both 14 CFR Parts 25 and 29, Appendix C ('typical' icing) and soon-to-be released Appendix O (supercooled large drop) conditions.

Nomenclature

CDP	Cloud Droplet Probe, drop sizer, 2 to 50 μm
CIP	Cloud Imaging Probe, drop sizer, 15 to 930 μm
DeltaP	Spray nozzle Pwat - Pair (psid)
Dv0.##	drop diameter at which ##% of the total volume of water is contained in smaller drops
FZDZ	Freezing Drizzle
FZRA	Freezing Rain
LWC	Liquid Water Content (g/m^3)
MVD	Median Volumetric Diameter (μm)
OAP-230X	Optical Array Probe, drop sizer, 15 to 450 μm
Pair	Spray nozzle atomizing air pressure (psig)
Pwat	Spray nozzle water pressure (psig)
SLD	Supercooled large drops
TWC	Total Water Content (g/m^3)
V	Calibrated true air speed (velocity) in the test section (kn)
μm	micrometer

Introduction

A calibration of the NASA Glenn Research Center Icing Research Tunnel (IRT) was performed between December 2013 and February 2014. The first step in this calibration process was to complete water flow coefficient tests of new spray nozzles. Once new nozzles were chosen, cloud calibration commenced with establishing a uniform cloud and calibrating the drop size and liquid water content. Transfer functions were developed to relate the inputs of air speed, spray bar atomizing air pressure and water pressure to the outputs of median volumetric drop diameter and liquid water content. This was done for both 14 CFR Parts 25 and 29, Appendix C (Refs. 1 and 2) ('typical' icing) and soon-to-be released Appendix O (supercooled large drop) conditions. The previous cloud calibration report was released in 2012, following the 2011 IRT heat exchanger and refrigeration plant upgrades (Ref. 3).

Facility Description

The IRT is a closed-loop refrigerated wind tunnel that simulates flight through an icing cloud. A plan view of the facility is shown Figure 1. A 5000-hp electric motor drives the 24-ft fan made of wood from Sitka spruce. The calibrated speed range in the test section ranges from 50 to 325 kn. The fan drives air through expanding turning vanes in "C-Corner", and into the face of the staggered heat exchanger. There, the air gets chilled/warmed within a temperature range of 20 °C total to -40 °C static. Twenty-four RTDs distributed on the D-Corner contracting turning vanes measure the total temperature. Several are visible in the inset picture. The heat exchanger is 26 ft high and 50 ft wide.

Downstream of the D-Corner contracting turning vanes are 10 rows of spray bars with two different air-atomizing nozzle types: Mod1 (lower water flow rates) and Standard (higher water flow rates). Each bar has 55 nozzle positions that contain either a Mod1 nozzle, a Standard nozzle or a plug. Each nozzle location is fed from two water manifolds through remotely controlled solenoid valves. It is possible to turn on only the Mod1 nozzles, only the Standard nozzles or both (with the same air pressure). The struts mounted vertically between spraybars that were required to help mix the cloud in 2006 are still necessary (Ref. 4).

The contraction area ratio into the test section is 14:1. The test section itself is 20-ft long by 6-ft high by 9-ft wide. The center of the test section is 44 ft from the spraybars. From the test section, the cloud flows into the diffuser toward A-Corner, and on around into B-Corner and into the fan.

Facility Change Notes

In preparation for the new icing cloud calibration, the Mod1 nozzle water tubes were replaced with new versions. A test stand was developed to perform water flow coefficient calibrations so that the new tubes could be tested and a set of nozzles could be selected with closely matching flow coefficients.

A set of nozzles with flow coefficients within 3 percent of the average were installed and used for this calibration effort. The plan had also been to replace the Standard nozzle water tubes as well. However, the flow coefficients for the new batch of Standard tubes were found to be 20 percent higher than the previous set. This would have increased the operating envelope gap between the Mod1 and Standard nozzles. The Standard tubes therefore were not replaced.

Icing Cloud Uniformity

Before the cloud characteristics of MVD and LWC can be determined, a uniform cloud must be established. This is determined by identifying which of the 550 possible nozzle locations should spray Mod1, which should spray Standard nozzles, and which should be plugged.

The diagnostic device is a 6×6 ft grid. This grid extends floor to ceiling, and covers the central 6-ft of the 9-ft span. The grid mesh is 6×6 in. Mesh elements are 2-in. deep with a flat 1/8-in. face for ice accretion. Digital calipers are used to measure the ice thickness accreted at the center mesh point of the vertical elements. An image of a technician measuring ice on the grid is shown in Figure 2.

The first step in developing a uniform cloud is to establish a nozzle transfer map. Single rows (i.e., spray bars) and columns of nozzles are sprayed to observe where ice accretes on the grid. This transfer map aids in the optimization of nozzle locations to produce a uniform cloud, and in the identification of problematic nozzles during routine testing.

To start the uniformity calibration, the previous January 2012 Standard nozzle pattern was loaded (Ref. 3), and still exhibited good uniformity over all airspeeds and drop sizes. A representative Standard nozzle uniformity pattern is shown in Figure 3; the legend indicates a ratio of the local LWC measured on the grid compared to the average of the central twelve values. The light green color shows most of the map is within ±10 percent.

The Mod1 nozzles were installed in a somewhat uniform pattern. Nozzles positions and number of nozzles were adjusted until a uniform icing cloud was developed on the icing grid. Since the majority of the IRT's models are airfoils mounted vertically and centered in the test section, greater care was taken to make the spanwise central –12 to 12 in. as uniform as possible. The Mod1 pattern was finalized with 88 spraying nozzles and 2 air-only nozzles. The LWC uniformity plots are shown in Figure 4 for four airspeeds at a drop size of 20 μm. Similar, but not shown, are the uniformity plots as a function of MVD. These can be made available to customers upon request.

Uniformity for a large drop case, MVD = 138 μm, is shown in Figure 5. Clearly, the vertical extent of the cloud is smaller than those in Figure 4, but the large drop uniformity is significantly improved over previous calibrations.

Drop Size Calibration

Drop Size Data Acquisition

In order to measure a complete drop size distribution, three instruments are sometimes needed. For the January 2014 drop-size calibration, these were the Cloud Droplet Probe, CDP (2 to 50 μm), Optical Array Probe, OAP-230X (15 to 450 μm) and Cloud Imaging Probe—Grayscale, CIP-GS or simply CIP in this document (15 to 930 μm). The IRT's OAP-230Y for the 50 to 1500 μm range was not functional at the time of testing. Figure 6 shows these probes mounted in the IRT test section. The OAP-230X was made by the Particle Measurement Systems, Inc. and is no longer being manufactured. The CDP and CIP were made by Droplet Measurement Technologies, Inc. (Boulder, CO). Through extensive testing in the IRT, it has been found that both these probes require considerable tuning to obtain reasonable data.

The CDP measures drop sizes between 2 to 50 μm in diameter using the Mie-scattering theory for forward-scattered light intensity. When a drop passes through the beam path of the CDP laser, it scatters light in all directions, and the forward-scattered light intensity is recorded by the probe and used to sort the drop size into one of 30 size bins. Since the CDP measures the smallest drop sizes of the three probes and since all spray conditions in the IRT contain small drops, data from the CDP is collected and used for the full range of spray conditions. Spray conditions ranged over the following: air pressures, Pair = 10 to 60 psig; delta pressures (water pressure minus air pressure), DeltaP = 5 to 250 psid for the Mod1 nozzles or 5 to 150 psid for the Standard nozzles.

Both the OAP-230X and the CIP measure drop size using a shadowing technique. Both probes have an array of photodiodes that are illuminated by a collimated laser beam. When a drop passes through the laser beam, the diodes that are shadowed to a certain threshold define the drop size. Data were taken with the OAP-230X for all spray conditions that produce a median volumetric diameter (MVD) greater than 18 μm. For this test, CIP usage was limited to larger drop conditions, Pair ≤ 8 psig.

Data Processing of Drop Size Distributions

An example drop size distribution is shown in Figure 7. The number density is the number of drops that are recorded in each bin normalized by its sample volume for that drop size and the bin width. The squares show the size distribution as measured by the CDP, and the triangles show the size distribution as measured by the OAP-230X. Note that the first three bins of the OAP-230X (the solid-black triangles) overlap with the CDP; these three OAP bins are not used in the drop size calculations.

The MVD is used to characterize the drop size distribution. This is the value at which half of the water volume is contained in smaller (or larger) drops; MVD is also referred to as $Dv0.5$. Correspondingly, $Dv0.9$ is the diameter at which 90 percent of the volume is contained in smaller drops. Normalized cumulative volume distributions for the IRT are shown in Figure 8. Bin volumes are plotted cumulatively, such that each data point represents the amount of water contained in all smaller diameters, normalized by the total volume contained in all bins. Figure 8(a) shows cumulative volume distributions for MVD values less than or equal to 50 μm and Figure 8(b) shows cumulative volume distributions for MVD greater than 50 μm .

Drop Size Equations

The MVD curve fit equations were determined by inputting the measured Pair, DeltaP and MVD into the curve fit generator TableCurve (Systat Software Inc.). The equations that were generated, while quite complex, fit the majority of the data within 10 percent, which is the typical target for the IRT. Different curve fits were generated for the Standard and Mod1 nozzles.

The Standard MVD curve fit equation is,

$$\text{MVD}_{\text{Standard}} = \frac{a + b * (\text{Pair}) + c * (\text{Pair})^2 + d * \ln(\text{DeltaP})}{1 + e * (\text{Pair}) + f * (\text{Pair})^2 + g * (\text{Pair})^3 + h * \ln(\text{DeltaP})} \quad (1)$$

where $a = 19.034$, $b = 0.0927$, $c = 0.00150$, $d = -3.945$, $e = 0.0474$, $f = -0.000669$, $g = 0.00000497$, $h = -0.438$.

The Mod1 MVD curve fit equation is

$$\text{MVD}_{\text{Mod1}} = a + b * (\text{Pair})^c + d * (\text{DeltaP})^e + f * (\text{Pair})^c * (\text{DeltaP})^e \quad (2)$$

where $a = 12.178$, $b = 267.014$, $c = -2.184$, $d = 0.00112$, $e = 1.362$, $f = 22.742$.

Figure 9 and Figure 10 summarize these MVD curve fits for Standard and Mod1 nozzles, respectively. In Figure 9(a) and Figure 10(a), the curve fit lines are plotted as a function of DeltaP for each calibrated Pair line. Measured MVDs are plotted against the respective curve fits for two Pair lines in each plot. Figure 9(b) and Figure 10(b) show how the curve fit values from the above equations compare to the measured values for all Standard and Mod1 conditions. The 1:1 line, as well as ± 10 percent lines are shown for reference. These plots show that the curve fits for the vast majority of the data points are within the IRT's typical targeted accuracy of 10 percent.

SLD in the IRT

A significant, current question is the IRT's ability to produce supercooled large drops or SLD. Larger drops are achievable by reducing the spray nozzle atomizing air pressure so there is less break up of the water stream. Operating the Mod1 nozzles between $2 \leq \text{Pair} \leq 8$ psig is referred to as "SLD" conditions in the IRT. To be clear, this short-hand phrase is mostly, but not fully technically accurate.

These SLD conditions were measured with the CDP and both the OAP-230X and CIP. Since the OAP-230X cannot measure drops larger than 450 μm , for the IRT nozzles its effective MVD limit is

175 μm . Previously, the CIP had been able to extend the range and returned values very similar to the OAP-230Y-combined distributions. During this calibration, however, there was a significant problem with the larger drops splashing or running off the CIP probe tips into the measurement volume. Until these difficulties can be overcome, the calibrated MVD range is limited to 175 μm . The MVD reported is the average of the CDP + OAP-230X and CDP + CIP that agreed within 10 percent. Note that the IRT has not lost the ability to produce its largest MVDs (historically up to 230 μm), only the ability to accurately characterize their diameter.

The measured Pair, DeltaP and averaged MVD values were put into the curve fit generator TableCurve (Systat Software Inc.). The SLD MVD (Mod1, $2 \leq \text{Pair} \leq 8$ psig) curve fit equation is

$$\text{MVD}_{\text{SLD}} = a + \frac{b}{\text{Pair}} + c * \text{DeltaP} + \frac{d}{\text{Pair}^2} + e * (\text{DeltaP})^2 + f * \frac{\text{DeltaP}}{\text{Pair}} \quad (3)$$

where $a = 6.5846$, $b = -92.6377$, $c = -1.7970$, $d = 341.4440$, $e = 0.007341$, and $f = 23.2670$.

Figure 11 summarizes the MVD curve fits for the SLD operating range. Figure 11(a) shows the curve fit lines as a function of DeltaP for each Pair line. Each of the measured MVDs are also plotted against their respective curve fits for all Pair lines. Figure 11(b) shows the MVD goodness of fit, plotting how the curve fit values (per Eq. (3)) compare to the measured MVD. The 1:1 line, as well as ± 10 percent lines are shown for reference. These plots show that the curve fit for these data points is well within the IRT's typical targeted accuracy of 20 percent for SLD conditions.

With the difficulty in measuring the largest MVDs, comparisons of the IRT distributions to the FAA Appendix O (Ref. 5) requirements are limited to freezing drizzle (FZDZ) conditions. These are seen in Figure 12 for FZDZ, $\text{MVD} < 40 \mu\text{m}$ and FZDZ, $\text{MVD} > 40 \mu\text{m}$. IRT distributions are selected that match the MVD (Dv0.5), or Dv0.98. Matching Dv0.9 (or similarly, Dv0.95 or Dv0.98) rather than the MVD would better assure that the effects of the larger drops in the distribution are captured.

Also recognize that FZDZ, $\text{MVD} < 40 \mu\text{m}$ conditions can be met with the more normal operation of $\text{Pair} > 10$ psig for the Mod1 nozzles. This is due to the fact that the IRT nozzles have long "tails"; that is, the largest drops produced for a spray condition are typically three to six times the MVD value.

Another concern with producing large drops in any facility is the ability to supercool them. A numerical and experimental study was conducted for and in the IRT (Ref. 6). Though the number of cases was limited, it found that 160 μm MVD drops (max drop size approximately 400 μm) at $V = 195$ mph were 1.9 F warmer than the static air temperature in the test section. As drop size increases, it can be expected that the difference between the drop temperature and the static air temperature will increase.

Liquid Water Content Calibration

Liquid Water Content Data Acquisition

A multi-wire instrument manufactured by Science Engineering Associates's (SEA; Mansfield Hollow, CT) was used to generate the liquid water content calibration (LWC). A picture of this instrument is shown in Figure 13. There are four elements within the anti-iced probe head. The three vertical elements (perpendicular to the flow) are a 0.5-mm wire, 2-mm cylindrical tube, and a 2-mm half-pipe element. The wire and cylindrical tube primarily measure LWC while the half pipe captures both LWC and ice particles (if present). The half-pipe measurement is therefore called total water content (TWC). The fourth element is a compensation wire which is placed behind the center element and parallel to the flow. It is designed to stay dry so that it tracks air temperature, air pressure and airspeed effects only. The four heated elements are held at a constant temperature of 140 $^{\circ}\text{C}$. The power required to maintain this temperature is proportional to the amount of water each element must evaporate. SEA defines the LWC calculation as (Ref. 7):

$$\text{LWC} \left(\frac{\text{g}}{\text{m}^3} \right) = \frac{C * P_{\text{sense,wet}}}{\left[L_{\text{evap}} + (T_{\text{evap}} - T_{\text{amb}}) \right] * V * L_{\text{sense}} * W_{\text{sense}}} \quad (4)$$

where $C = 2.389 * 10^5$, $P_{\text{sense,wet}} = P_{\text{sense,total}} - P_{\text{comp}} =$ wet power (W) measured by the sense element, $L_{\text{evap}} =$ latent heat of evaporation (cal/g), $T_{\text{evap}} =$ evaporative temperature (C), $T_{\text{amb}} =$ ambient static temperature (C), L_{sense} and $W_{\text{sense}} =$ length and width respectively of the sense element (mm) and $V =$ true airspeed (m/s). $P_{\text{sense,total}}$ is the total power measured by the element, P_{comp} is the power measured by the compensation element.

The half-pipe is the primary sensor used in the IRT for LWC measurements. A collection efficiency correction for this element was determined and applied for analysis. The collection efficiency is a function of airspeed, drop size and geometry. For this design, E_b was calculated by the FWG two-dimensional particle trajectory code (Ref. 8).

Liquid Water Content Equations

The data from the multi-wire were compiled to build the LWC curve fits, correlating liquid water content to P_{air} , ΔP , and V . As described in the 2006 IRT calibration report (Ref. 4), the liquid water content calibration is a function of the form:

$$\text{LWC} = K(V, P_{\text{air}}) * \frac{\sqrt{\Delta P}}{V} \quad (5)$$

where K is a function of velocity and P_{air} . The first step of fitting the LWC curve is to determine the function K for both parameters, “ K_v ” and “ K_a ”. To do this, measurements were made from $V = 50$ to 325 kn while P_{air} and ΔP (and MVD) are held constant, defining K_v . K_a is defined by holding velocity and MVD constant while making measurements from $P_{\text{air}} = 10$ to 60 psig. K is calculated for each of these measured values based on the above relationship: $K = \text{LWC} * V / \sqrt{\Delta P}$. Figure 14 shows the linear relationships that were found when K was correlated to velocity and P_{air} for both Mod1 and Standard nozzles. These linear fits are combined to determine the planar function K . An additional correction factor was added after it became apparent that even with this curve fit optimized, there was a clear correlation of LWC to MVD for both the Mod1 and Standard nozzle sets. From this, the expected curve is of the following form:

$$\text{LWC}_{\text{Mod1}} = (a * V + b * P_{\text{air}} + c) * \left(\frac{\text{MVD}}{d} \right)^e * \frac{\sqrt{\Delta P}}{V} \quad (6)$$

where a is the slope of the K_v versus V line, b is the slope of the K_a v P_{air} line, d is a basis MVD and c and e are constants.

A MATLAB code was written that would optimize a curve fit in this specific format. For the Mod1 nozzles, the curve fit predicted the measured values within ± 10 percent, as shown in Figure 15(a). The LWC curve fit equation for Mod1 nozzles in Appendix C conditions follows the above form, with $a = 0.02989$, $b = -0.050414$, $c = 9.519$, $d = 21.6256$, $e = 0.18306$.

The Standard LWC curve fit is similar, but with a DeltaP correction that was found to improve the fit of the curve. The LWC curve fit for Standard nozzles is

$$LWC_{\text{Standard}} = (a * V + b * \text{Pair} + c) * \left(\frac{\text{MVD}}{d} \right)^e * \frac{\sqrt{\text{DeltaP} - 1}}{V} \quad (7)$$

where $a = 0.156$, $b = -0.25$, $c = 44$, $d = 22$, $e = 0.17$. The goodness of fit for this equation is shown in Figure 15(b), which plots the predicted curve fit values against the measured values.

The LWC curve fit equations for SLD conditions (Mod1 , $2 \leq \text{Pair} \leq 8$ psig) were determined by inputting the measured Pair, DeltaP and LWC into the curve fit generator TableCurve (Systat Software Inc.). Because of the parameter limitations of the software, one curve was created for the basis velocity value, and then a velocity correction was applied so the equation would account for the velocity dependency of LWC.

The LWC curve fit for SLD conditions is

$$LWC_{\text{SLD}} = \left(a + \frac{b}{\text{Pair}} + c * \text{DeltaP} + \frac{d}{\text{Pair}^2} + e * \text{DeltaP}^2 + f * \frac{\text{DeltaP}}{\text{Pair}} + \frac{g}{\text{Pair}^3} + h * \frac{\text{DeltaP}^2}{\text{Pair}} + i * \frac{\text{DeltaP}}{\text{Pair}^2} \right) * \left(\frac{V}{k} \right)^m \quad (8)$$

where $a = 0.1871$, $b = -0.2469$, $c = 0.00173$, $d = -0.0396$, $e = 0.000107$, $f = 0.1058$, $g = 0.6597$, $h = -0.000713$, $i = -0.0830$, $k = 148$, and $m = -0.75$. The goodness of fit for this equation is shown in Figure 15(c), which plots the predicted curve fit values against the measured values.

Figure 15 shows that the curve fits agree with the majority of the data within 10 percent, even for SLD conditions, which have a target accuracy of 20 percent.

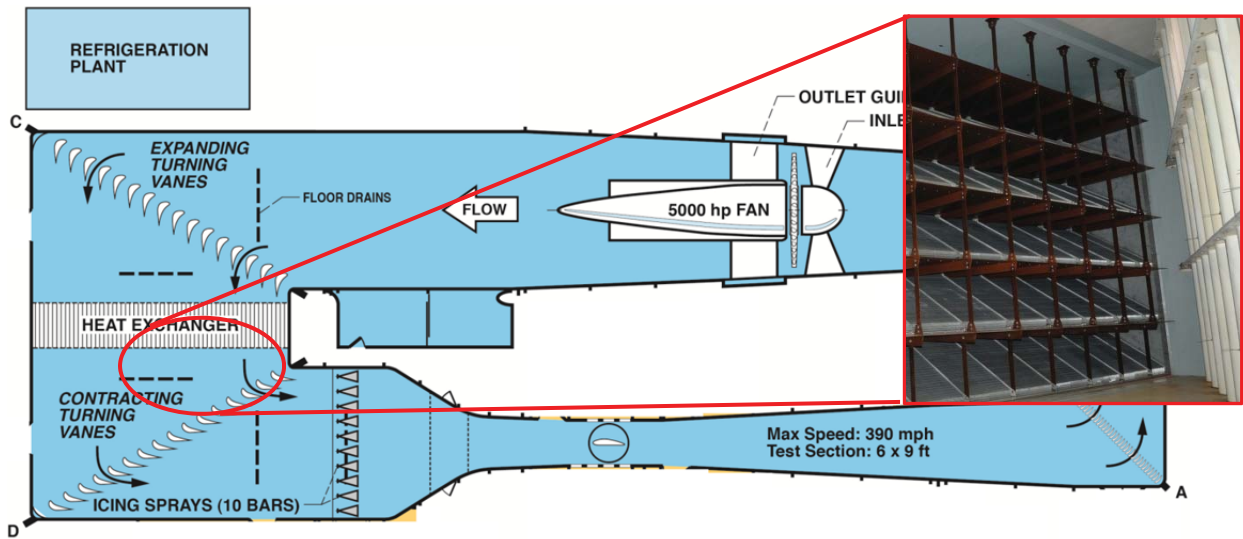
Icing Cloud Operating Ranges

The IRT's icing envelopes for both the Mod1 and Standard nozzles are compared to the FAA Appendix C icing criteria in Figure 16. The airspeed of 225 kn is selected. At lower air speeds, the curves shift up to higher LWC, at higher air speeds they shift down. While the commonly requested data points $\text{MVD} = 20 \mu\text{m}$, $\text{LWC} = 0.5$ and 1 g/m^3 are easily achieved, another requested point, $\text{MVD} = 40 \mu\text{m}$, $\text{LWC} = 0.07 \text{ g/m}^3$ will likely never be achieved with the current nozzle design. The operating envelopes for the SLD conditions of Mod1 at $2 \leq \text{Pair} \leq 8$ psig are shown in Figure 17. The maximum and minimum calibrated velocities are plotted. Also indicated are the range of temperature-dependent maximum LWC values for each freezing drizzle environmental condition of Appendix O (per Fig. 1 in Ref. 9).

Conclusion

The procedures and results of the full cloud calibration that was conducted in NASA Glenn's Icing Research Tunnel from December 2013 to February 2014 have been described. The calibration followed the installation of a new set of Mod1 nozzles that had a tighter range of water flow coefficients.

Uniform icing clouds were established with both the Standard and Mod1 nozzles. The MVD and LWC curve fits for both the Standard and Mod1 nozzle sets are within the ± 10 percent targets. For SLD conditions, the calibrated MVD range is limited to $175 \mu\text{m}$, until such time that the difficulties in measuring the largest drops the IRT can produce can be overcome. The SLD MVD and LWC curve fits were well within the ± 20 percent targets, coming in around ± 10 percent.



CD-10-83244c

Figure 1.—A plan view schematic of the Icing Research Tunnel. Inset: View of the staggered heat exchanger and inner D-Corner turning vanes, flow is left to right.



Figure 2.—A technician measures the thickness of ice accreted on the grid.

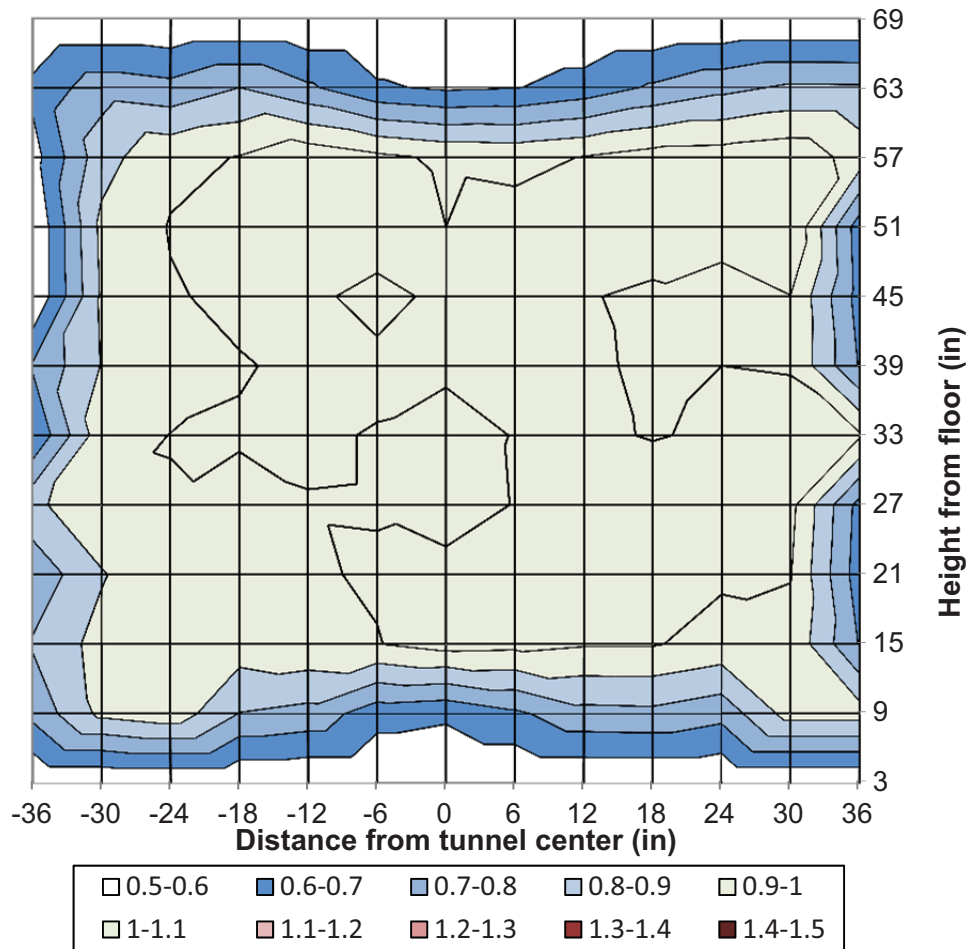


Figure 3.—LWC uniformity contour plot for the standard nozzles, $V = 150$ kn, $MVD = 20 \mu\text{m}$, $P_{air} = 15$ psig.

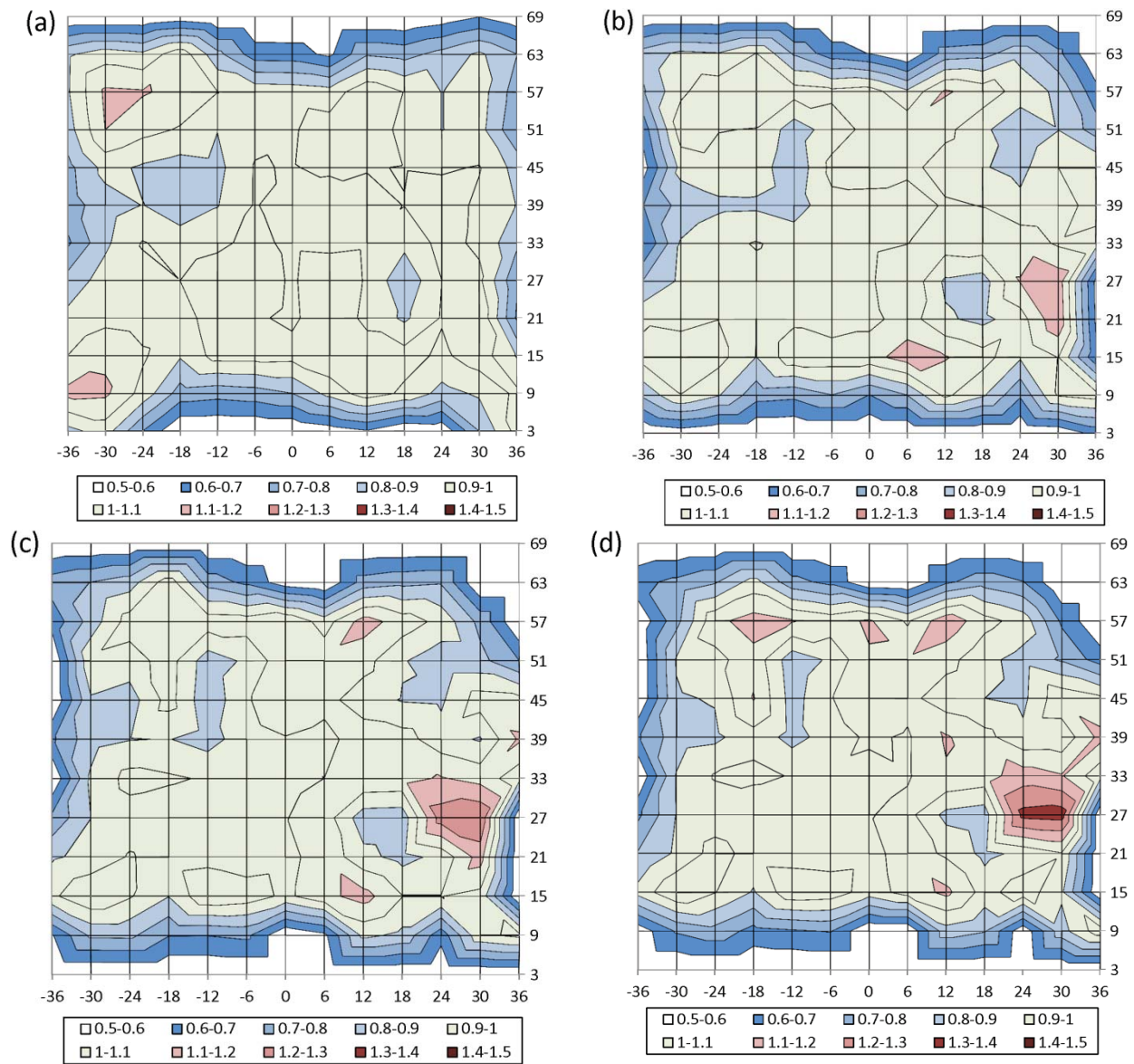


Figure 4.—Mod1 nozzle LWC uniformity plots for several airspeeds, MVD = 20 μm , Pair = 20 psig, V = (a) 100 kn, (b) 150 kn, (c) 200 kn, (d) 250 kn (Axes same as Figure 3).

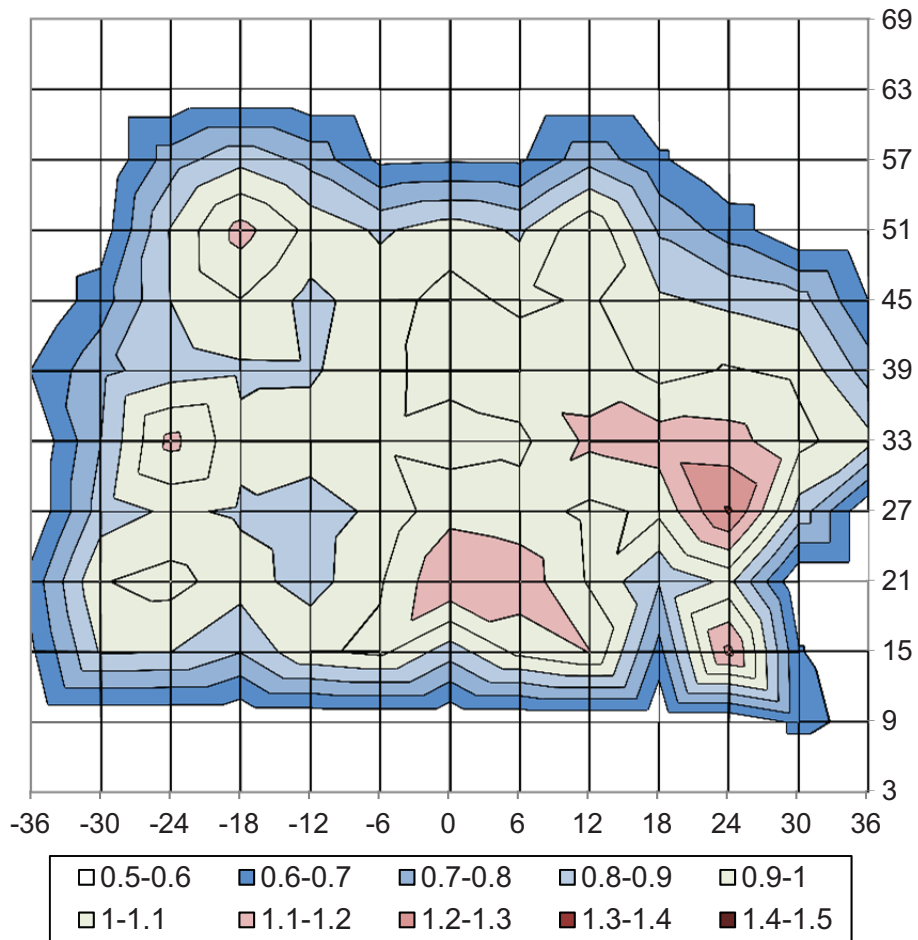


Figure 5.—LWC uniformity contour plot for an SLD case, $V = 150$ kn, $MVD = 138 \mu\text{m}$, $\text{Pair} = 3$ psig. (Axes same as Figure 3).

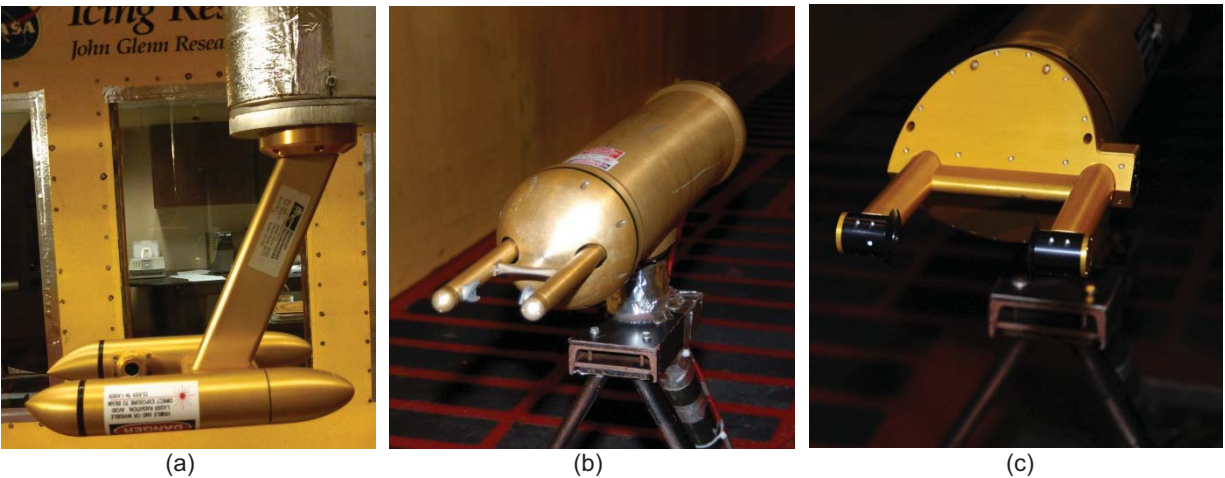


Figure 6.—Images of drop-sizing probes used for calibration in the IRT: (a) Cloud Droplet Probe (CDP), (b) Optical Array Probe (OAP-230X), (c) Cloud Imaging Probe-Grayscale (CIP-GS).

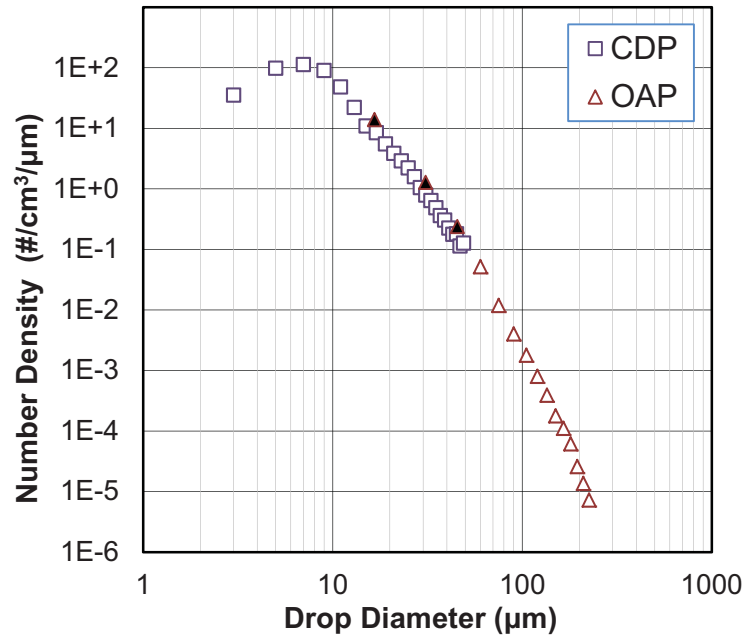


Figure 7.—Drop size distribution presented as number density versus drop diameter, measured by the CDP + OAP-230X, MVD = 25 μm .

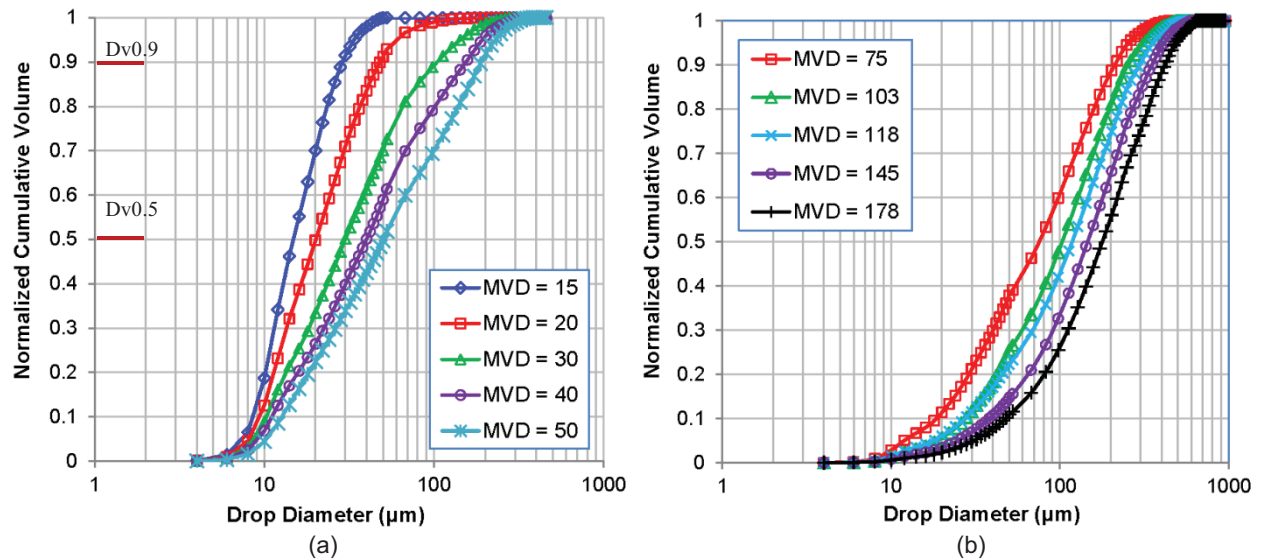


Figure 8.—Cumulative volume distributions: (a) MVD $\leq 50 \mu\text{m}$ with Dv0.5 (= MVD) and Dv0.9 indicated, (b) MVD $> 50 \mu\text{m}$.

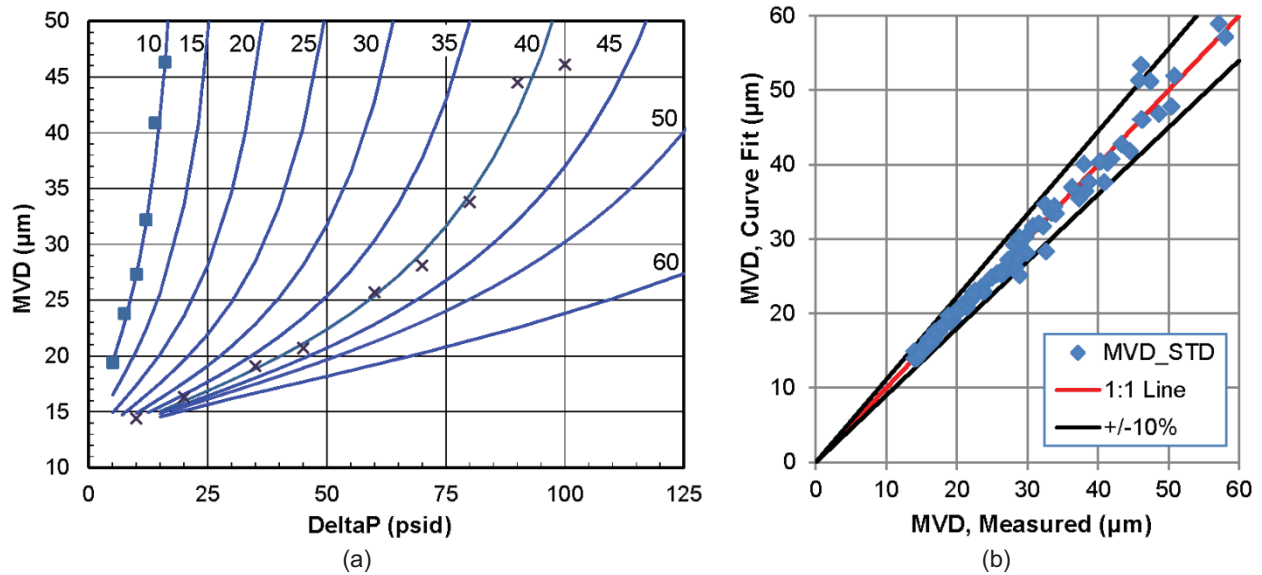


Figure 9.—Drop size calibration curves for the Standard Nozzles: (a) MVD versus DeltaP for each (labeled) Pair line. The curves are the fit. The measured MVD for Pair = 10 and 40 psig lines are also plotted as data points. (b) Curve fit versus measured MVD for all Standard-nozzle calibration points.

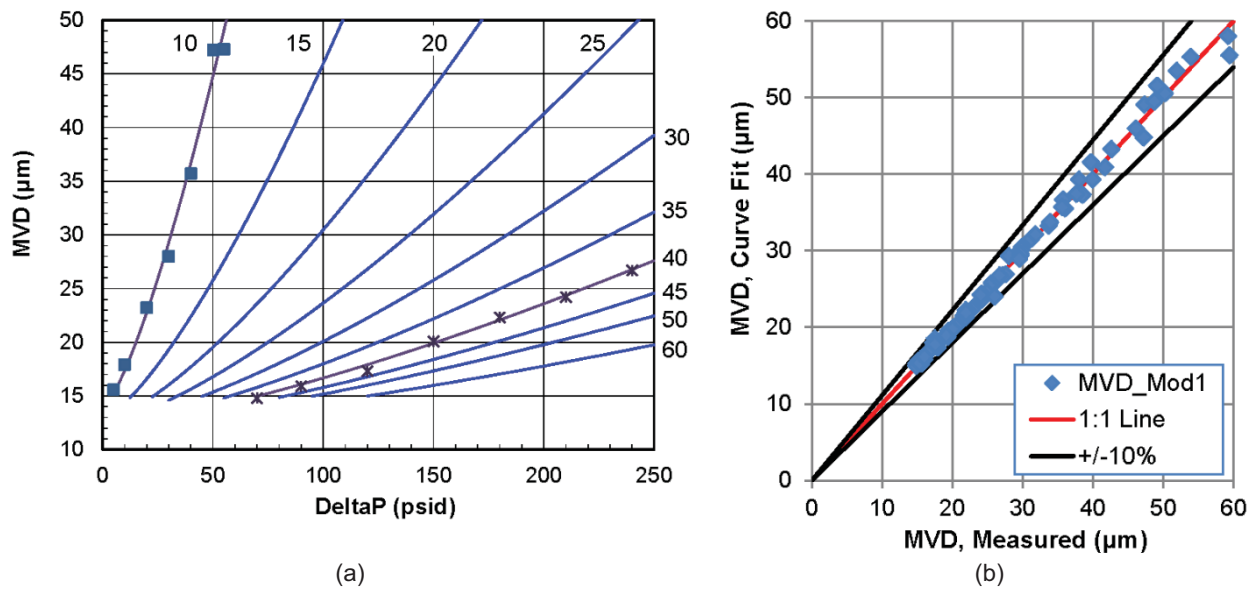


Figure 10.—Drop size calibration curves for the Mod1 Nozzles: (a) MVD versus DeltaP for each (labeled) Pair line. The curves are the fit. The measured MVD for Pair = 10 and 40 psig lines are also plotted as data points. (b) Curve fit versus measured MVD for all Mod1-nozzle calibration points.

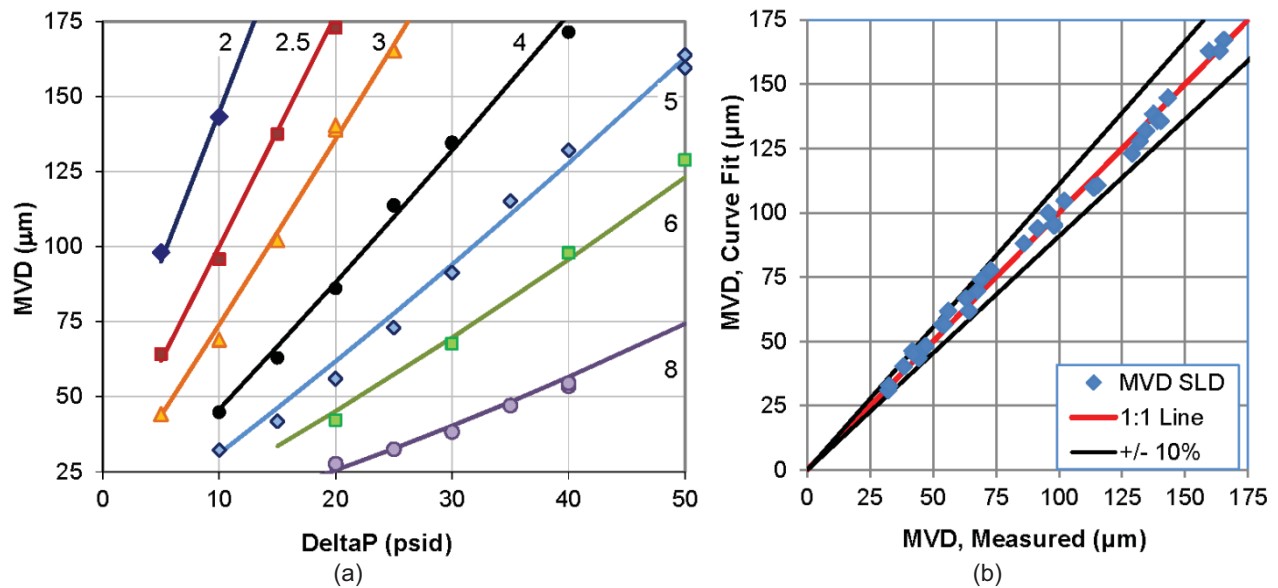


Figure 11.—Drop size calibration curves for SLD conditions (Mod1 nozzles, Pair \leq 8 psig): (a) MVD versus DeltaP for each (labeled) Pair line. The curves are the fit. The measured MVD for each Pair line are also plotted as data points. (b) Curve fit versus measured MVD for all SLD calibration points.

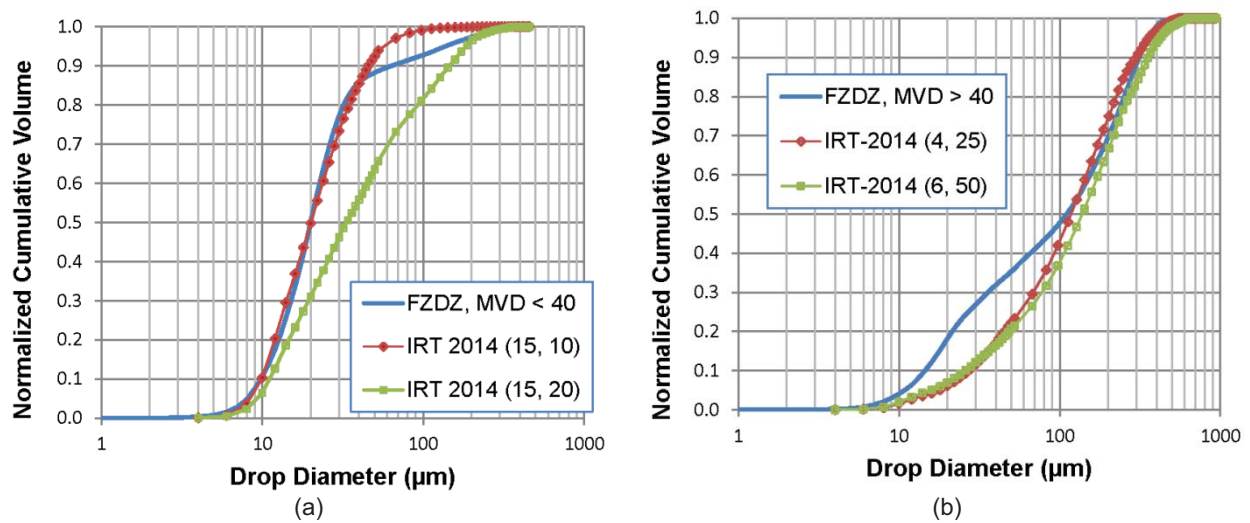
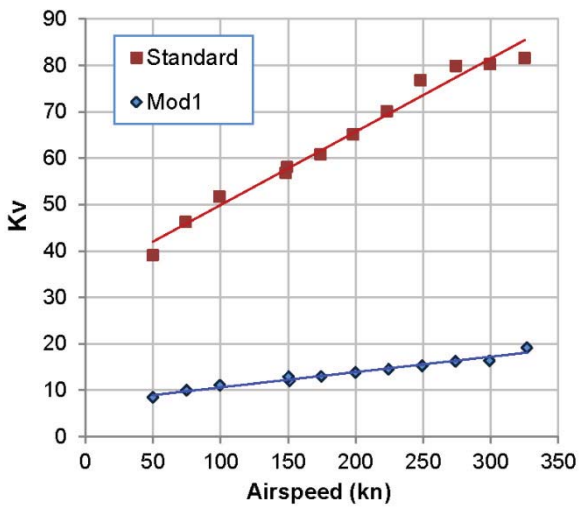


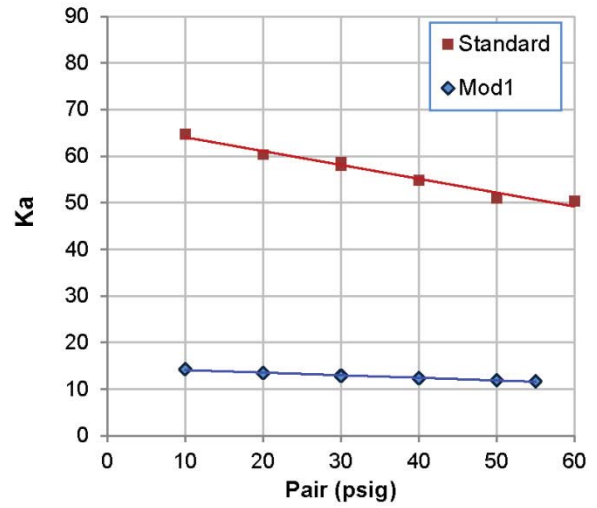
Figure 12.—Comparison of IRT distributions to proposed FAA Appendix O conditions for FZDZ: (a) MVD < 40 μm , (b) MVD > 40 μm .



Figure 13.—The Multi-wire liquid water content instrument mounted in the icing tunnel.



(a)



(b)

Figure 14.—LWC parameters, K, for the Standard and Mod1 nozzle sets showing the effect of (a) Kv versus airspeed, and (b) Ka versus Pair.

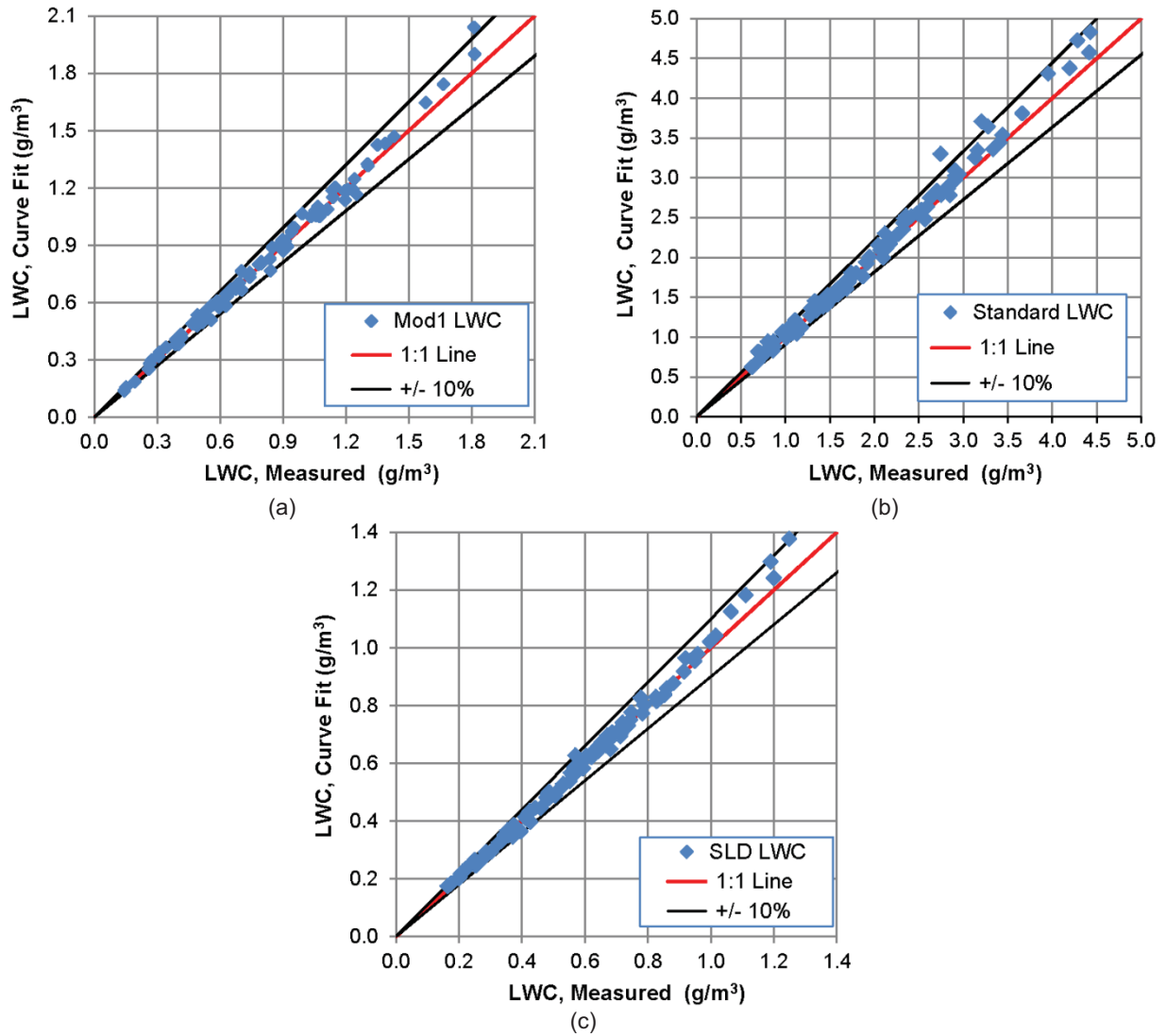


Figure 15.—A comparison of the curve fit versus measured LWC at all calibrated conditions for (a) Mod1 nozzles, (b) Standard nozzles, (c) SLD conditions.

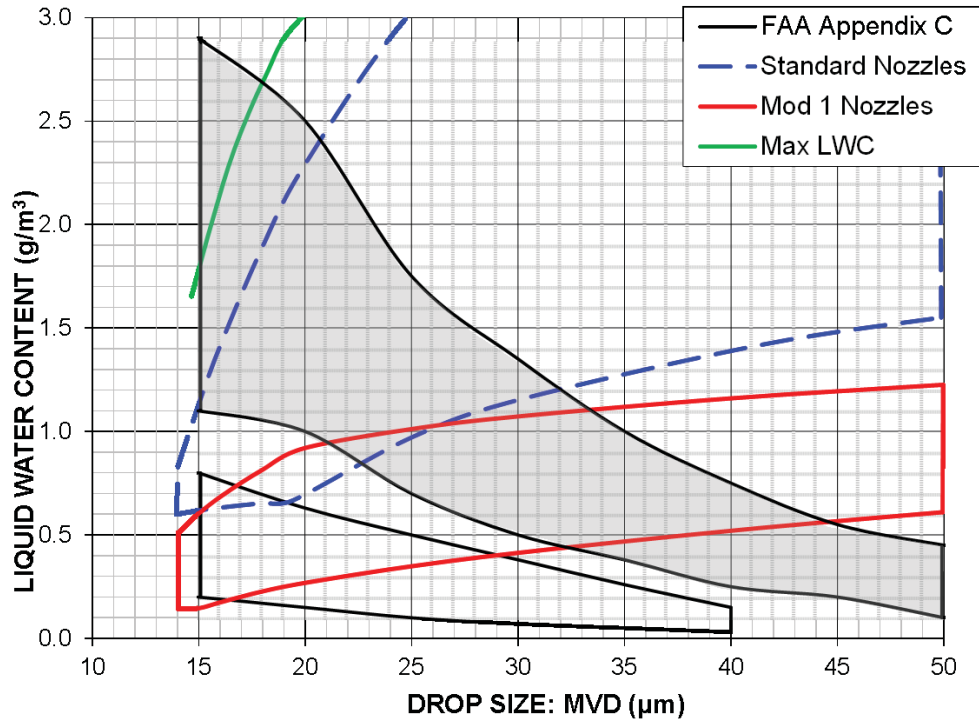


Figure 16.—Comparison of the IRT operating envelopes, LWC versus MVD, to the FAA Icing Certification criteria for an airspeed of 225 kn. The FAA Appendix C envelopes are shaded and indicated in black. The Mod1 nozzles are in red and the Standard nozzles are in dashed blue. The Mod1 and Standard nozzles can be combined under limited circumstances to produce higher LWC, shown in green.

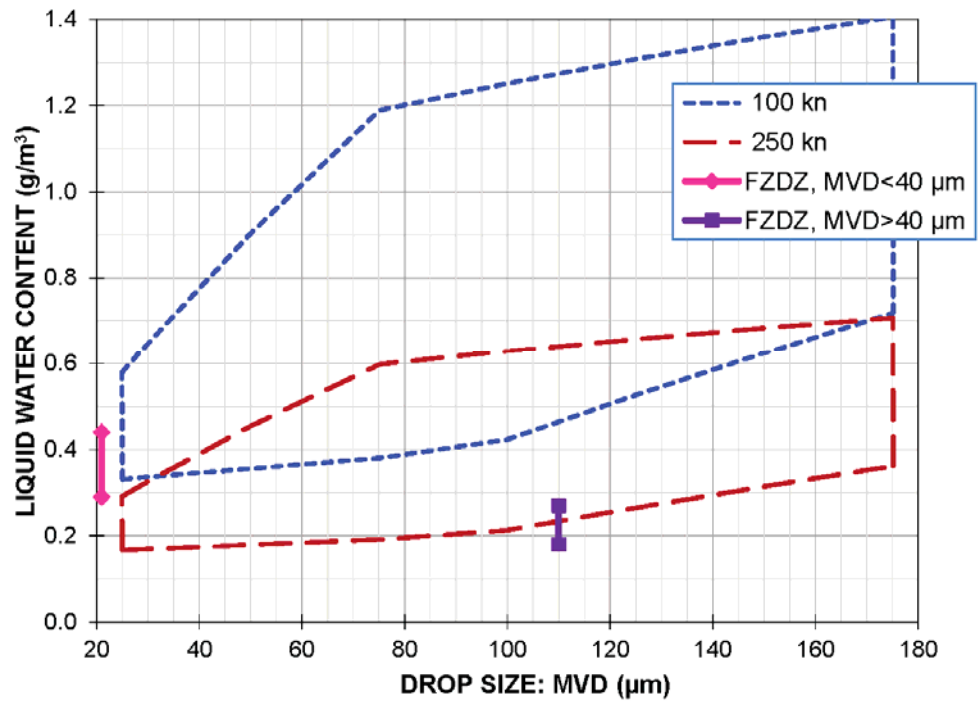


Figure 17.—The IRT SLD operating envelopes at $V = 100$ and 250 kn. (Pair between 2.0 and 8.0 psig.) For reference, the Appendix O max LWC ranges are also shown for each FZDZ condition, per Figure 1 of Reference 9.

References

1. CFR 14, Part 25, Appendix C, “Atmospheric Icing Conditions,” <http://www.ecfr.gov/cgi-bin/text-idx?SID=90a70d57d146d0a7dfecb6d394f2c2d0&node=14:1.0.1.3.11&rgn=div5#14:1.0.1.3.11.9.201.2.19> accessed on 3/18/2014, updated annually.
2. Jeck, Richard K., “Icing Design Envelopes (14 CFR Parts 25 and 29, Appendix C) Converted to a Distance-Based Format,” DOT/FAA/AR-00/30, Apr 2002.
3. Van Zante, Judith F., Ide, Robert F., Steen, Laura E., “NASA Glenn Icing Research Tunnel: 2012 Cloud Calibration Procedure and Results,” 4th AIAA Atmospheric and Space Environments Conference, New Orleans, Jun 2012.
4. Ide, Robert F., Sheldon, David W., “2006 Icing Cloud Calibration of the NASA Glenn Icing Research Tunnel,” NASA/TM—2008-215177, May 2008.
5. FAA FAR 14 CFR Parts 25 and 33, “Airplane and Engine Certification Requirements in Supercooled Large Drop, Mixed Phase, and Ice Crystal Icing Conditions,” Federal Register / Vol. 75, No. 124 /Tuesday, June 29, 2010/Proposed Rules.
6. Miller, Dean R., Addy, Harold E., Ide, Robert F., “A Study of Large Droplet Ice Accretions in the NASA Glenn IRT at Near-Freezing Conditions,” NASA/TM—1996-107142/REV1, ARL–MR–294, AIAA–96–0934, June 2005.
7. Science Engineering Associates, “WCM-2000 Users Guide,” <http://www.scieng.com/> Oct 6, 2010.
8. Frost, W., “Two-Dimensional Particle Trajectory Computer Program,” Interim Report for Contract NAS3–22448, Mar. 1982.
9. Cober, S. Bernstein, B., Jeck, R., Hill, E., Isaac, G., Riley, J., and Shah, A., “Data and Analysis for the Development of an Engineering Standard for Supercooled Large Drop Conditions,” DOT/FAA/AR-09/10, Mar 2009.

